Proceedings of the 30th Asia-Pacific Advanced Network Meeting

Population detection profiles of DMSP-OLS night-time imagery by regions of the world

Christopher N.H. DOLL [1,2]*

1 United Nations University – Institute of Advanced Studies, 1-1-1 Minato Mirai, Yokohama Kanagawa-ku, 220-8502, JAPAN
2 Department of Urban Engineering, The University of Tokyo, 7-3-1 Hongo, Bunkyo-ku, Tokyo, 113-8656, JAPAN

E-Mail: doll@ias.unu.edu

* Author to whom correspondence should be addressed;

Tel.: +81-45-221-2342; Fax: +81-45-221-2302

Abstract: One emerging application of night-time light imagery focuses on estimating levels of access to electricity globally (Doll & Pachauri, 2010; Elvidge *et al.*, 2010). A central consideration of such studies is the population density which can be consistently detected from night-time light imagery. Whilst numerous studies have addressed the relationship to light and population statistics in order to predict population, the use of spatially explicit population databases allows for a more detailed description of these relationships. This paper reports the variation of different detection profiles of two publically available gridded population datasets. These are disaggregated by region to reveal a vast contrast in what we may assume to be observable population in different parts of the world. A dynamic trend emerges with respect to levels of development with the most developed nations hypothesized to be the theoretical minimum observable population density. Beyond contributing to the analysis of areas of the world without access to electricity, more fundamentally, this analysis addresses a basic question about night-time lights and how it relates to population globally and in particular the relative merits of two commonly used population databases.

Keywords: DMSP-OLS night-time lights; population; regions.

---

1. Introduction

One of the most intuitive uses of night-time light satellite imagery is to use it as a proxy for the location of human population. The global coverage of anthropogenic light emissions presents an image of human activity which has a great visual impact to both lay and professional observers. As a measure of development it is striking both in what it shows and what is absent. Comparing the spatial distribution of light emissions to that of human population reveals the short comings of using night-time lights as an absolute proxy for the location of human settlements. Large parts of the developing world remain without access to electricity despite sizable populations. Nonetheless studies have shown the utility of night-time lights to be a descriptor of urban location and urban population (Sutton et al., 2001). More recently, studies have focused on whether night-time light imagery can be used to assess levels of access to electricity (Doll and Pachauri, 2010; Elvidge et al., 2010). An obstacle in undertaking such studies is that an appreciation or estimate of the level of population which goes undetected is helpful to interpret the results. Given the very wide range of levels of development and use of lighting across the world, this study seeks understand what level of population can be detected in different regions of the world. Furthermore, this paper assesses the difference between datasets of residential and ambient population. Residential population is what traditionally has always been recorded in national censuses. It essentially records where people live. Whilst this has advantages in many areas, not least data collection, it is less useful in certain applications of demography which require information on where people may actually be during the day. This is termed ambient population and refers to, for example, the population of downtown areas during the day or other loci which experience diurnal fluctuations. It has applications in many areas such as disaster management: what is the exposed population when an earthquake strikes during the mid-morning?

Ambient population is decidedly more difficult to estimate because it relies on a number of factors such as the density of transport networks to transport people into an area (itself a location of ambient population), the available building stock to accommodate the influx of people into an area and so on. Sutton et al. (2003) describes a number of approaches to model this distribution which they characterize as a temporally averaged measure of population density taking into account where people sleep, work, eat and so on.

Whilst studies have taken statistical data and compared night-lights at various administrative levels from national to local to pixel (Sutton et al., 2001; 1997), a pixel by pixel analysis is

decidedly more difficult owing in part to the uncertainties present in the night-time lights dataset and the fact that light emissions are not solely a function of population and are in fact strongly dependent on economic activity (Raupach et al., 2010). This study does not concern itself with the pixel to pixel correspondence but rather takes a broader approach to understand what is the likelihood of a pixel appearing lit at a given population density and given the wide range of economic development across the world, what is the magnitude of the difference in the relationship between light intensity and population density by region. Such information is useful not only from the standpoint of understanding the characteristics of night-time light data from the DMSP-OLS sensor but also the difference between the two population datasets considered in this study.

2. Approach

Using the spatial analysis functions in ArcGIS, DMSP-OLS night-time light imagery was overlaid with two spatially explicit population datasets. The two population datasets used in this study are both publicly available but differ slightly in their methodology. In this sense they are not directly comparable for analyzing the change in population detection in a given region over time but rather to highlight the differences within a region between residential and ambient population. The regional definitions used for this study is a 11 region political-economic classification from the International Institute for Applied Systems Analysis precise details of which can be found here (IIASA, 2006).

2.1. Description of datasets used in the study

2.1.1. DMSP-OLS Night-time lights

The night-time light satellite imagery comes from the current latest public release of the annual stable lights composite (version 4) of the Defense Meteorological Satellite Program's Operational Linescan System (DMSP-OLS) the National Oceanic and Atmospheric Administration's National Geophysical Data Center (NOAA-NGDC, 2010). The stable lights dataset is an annual composite of numerous night-time scenes taken throughout the year of production. DMSP-OLS was originally conceived as a meteorological satellite designed to observe clouds at night. Over time it has been realized that it also observes a number of other human activities through surface light emissions under cloud free conditions. The sensor itself has a resolution of 2.7km with two bands one in the visible-near infrared (0.4-1.1μm) and the other in the thermal band (10.5-12.6μm).

The combined used of these bands allows detailed description of light emissions to be produced. Taking data from scenes of low lunar illumination and using the thermal band to distinguish clouds from surface lights, a complex mosaic of images is sequentially built which, using a sequence of geolocation and compositing algorithms are processed to produce a seamless image which records the average digital number (DN) of consistently present (stable) lights throughout the year at 30arc-second resolution (~1km at the equator). A full description of the sensor characteristics and processing algorithms can be found in Elvidge et al (1997; 2001). As new satellites are launched to replace the old sensors, there may be more than one dataset available for any given year. Currently there are 30 datasets of annual composited data available for the years 1992-2009. For this study, the composites from the F14 sensor for 2000 and the F16's 2008 product were used to match the years of the corresponding population dataset.

There are a number of known issues with the DMSP-OLS night-time lights dataset, knowledge of which is helpful when interpreting results. Firstly is that due to the spatial configuration of the sensor, the dataset tend to overestimate the aerial contribution of light. This can happen in two ways. One is due to the coarse resolution and high sensitivity of the sensor, light can be detected from feint sources which may not cover the entire pixel. Secondly, pixels that appear to be lit may not have a light source due to atmospheric scattering from adjacent pixels. This is termed overglow The high sensitivity of the sensor combined with the low dynamic range leads to a second issue, that of sensor saturation. It is often the case that over bright urban areas, the maximum DN value (63) is reached. Whilst techniques to help overcome this have been discussed (Elvidge et al., 1999; Small et al., 2005) these are not applied to the stable lights dataset used in this study.

2.1.2. CIESIN GRUMP & LandScan Population datasets

The two population datasets used are both gridded at 30-arc second resolution. The first is the Global Rural Urban Mapping Project (GRUMP) from the Center for International Earth Science Information Network (CIESIN) (CIESIN et al, 2004). This population dataset takes 2000 census data from 1 million administrative units to produce a global gridded population data product. It is further enhanced by using a global database of urban settlements to model urban-rural population and then weighting population to urban areas. This database is largely derived from an earlier version of the night-time lights dataset (1994-95) but is augmented with data from the Digital Chart of the World and tactical pilotage charts in order cover areas which may not appear in night-time light imagery. In these cases a delimitation of urban area is achieved by using the

population data to derive an areal extent based on an allometric growth function. The urban settlements layer is used give larger weight to urban areas than rural areas when population is allocated to each cell. Whilst this may not have a noticeable effect in areas where the urban settlement is larger than the administrative area, it will be significant where urban areas intersect or lie within administrative units. In doing so, it aims to achieve a more accurate representation of population than through census areas alone.

The LandScan (LandScan, 2008) population dataset refers to global population from 2008 and is the product of a more complicated data input stream. Previous versions also relied on night-time light imagery but it was determined that the nighttime lights were more representative of economic activity (Bhaduri et al., 2002) and has subsequently been replaced with a suite of ancillary land cover data. In addition to the census population and administrative area statistics, data on land-cover data, slope, elevation, road networks, urban boundaries and other populated points as well as coastlines are all combined to produce a population probability grid which maps the likelihood of population appearing in a cell. Further modifications to this coefficient are made by analyzing high-resolution imagery to assess factors like building density and settlement patterns in urban areas (ORNL, 2010). This leads to what is known as 'ambient population'. The product is a more precise representation of population based on a calculation of the likelihood of population appearing in a cell based on a weighted combination of the aforementioned factors.

As a point of note, the accuracy either relative or absolute of either dataset is unknown and despite the enhanced precision of the LandScan dataset, no assessment of accuracy is claimed or acknowledged for either dataset. Indeed it is not the purpose of this study to determine which dataset is better or more accurate but merely to assess the characteristics of each dataset with respect to night-time light imagery.

2.2. Methodology

Initially we consider the ratio of areas which are unlit to lit as a measure of the likelihood of population detection. This is done by using a binary mask to exclude lit areas and then, for each region, obtaining the population density profile (i.e. for unlit areas). This is then compared to the population density profile of the entire scene to get the proportion of unlit pixels in each population density class. When plotted out together a series of detection profiles are generated for each region, which describes the how light detection varies with population density for each dataset. We expect to see that different regions will exhibit different profiles and this should fit with a simple conceptual model that more developed regions have higher levels of light detection

for a given population density (i.e. low ratio of unlit:lit cells). These profiles are arranged by regional groups and shown in Figures 1-3.

The analysis then moves on to describe the relationship between population density and light intensity. This part of the analysis deals with the population density within lit regions of the world. In essence, the first part of the analysis determined the population density profile in areas with no light (DN=0). Clearly, similar population density profiles exist for each DN value. The second part of the analysis condenses these profiles into a representative single population density value for each DN value by calculating the weighted average of population density in for each DN value. The weighted average of population density (*PopD*) for any given DN value was calculated according to the equation (1). The two graphs showing DN vs. average population density for LandScan and GRUMP datasets are shown in Figure 4.

$$PopD = \frac{\sum_{i=1}^{n} PopD_i \times Cells_i}{\sum_n Cells} \tag{1}$$

Where: $PopD_i$ = Population density of value *i*
Cells = the number of cells in a given population density class

Taken together, these two analyses build a comprehensive overview of the regional differences in population detection in both lit and unlit areas disaggregated by regions of the world.

3. Results

3.1. Population density profiles in unlit areas

The graphs presented in this section plot the relationship between unlit cells and population density. This variation of population detection in unlit areas is constructed for each of the 11 regions defined in the study. These are presented here grouped according to general levels of development. Figure 1 shows the relationship for the North American, Pacific OECD, Western and Eastern Europe. This first three in the group represents the most economically developed set of countries and their profile in unlit areas is that of sharp decline in unlit areas, such that only around 10% of cells are in unlit areas at 30persons.km^{-2}. The decline is sharpest for North America where both datasets show consistent detection (> 95%) at this population density.

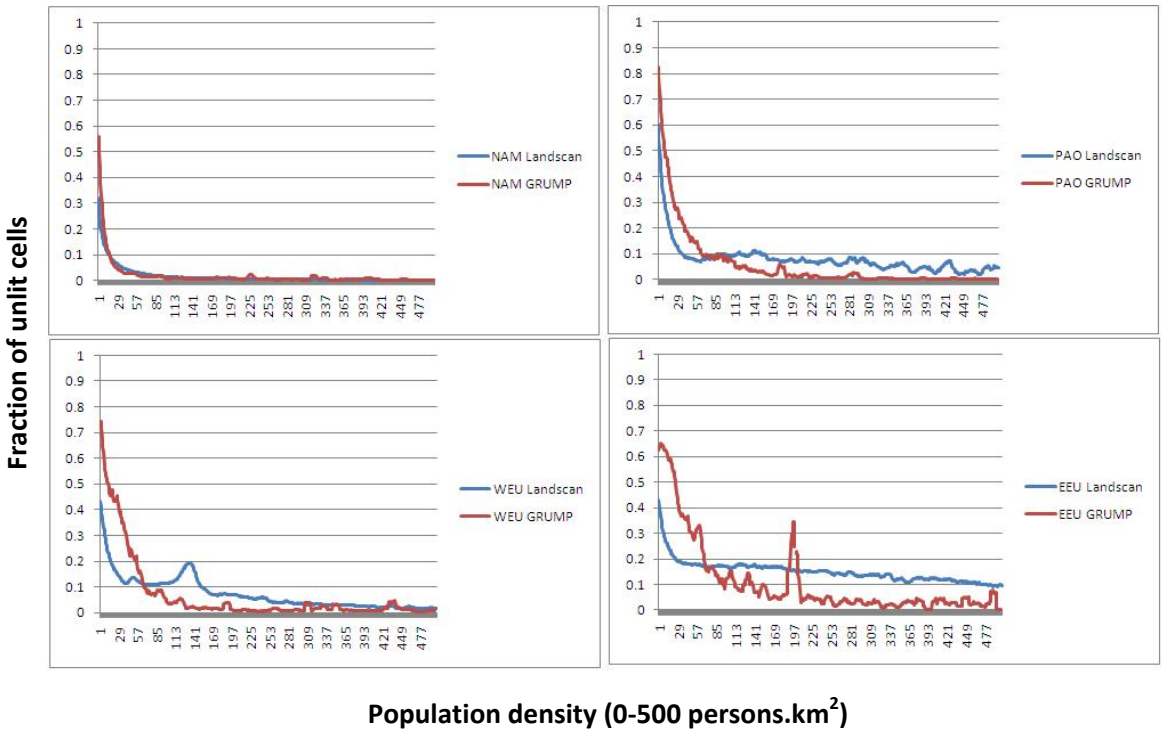

Figure 1. Population density detection profile for four regions. Clockwise from top left: NAM – North America; PAO – Pacific OECD; EEU – Eastern Europe; WEU Western Europe.

Figure 2 shows the result for the least developed regions of the world. Sub-Saharan Africa and Pacific Asia display markedly different profiles between the two population datasets. In both cases, there is a higher level of cells which are undetected in the LandScan dataset than with the GRUMP dataset. Pacific Asia can be seen to be consistently detected at 90% levels from around 700 persons.km^{-2} in GRUMP compared to 60% in LandScan, whilst the decline in the proportion of unlit cells is much more gradual for sub-Saharan Africa with 35% of cells unlit at 1000 persons.km^{-2} in the GRUMP dataset and 75% in LandScan. The profiles are much more similar for Latin America both falling with GRUMP again ahead of LandScan but both achieving 80% detection at 500 persons.km^{-2}.

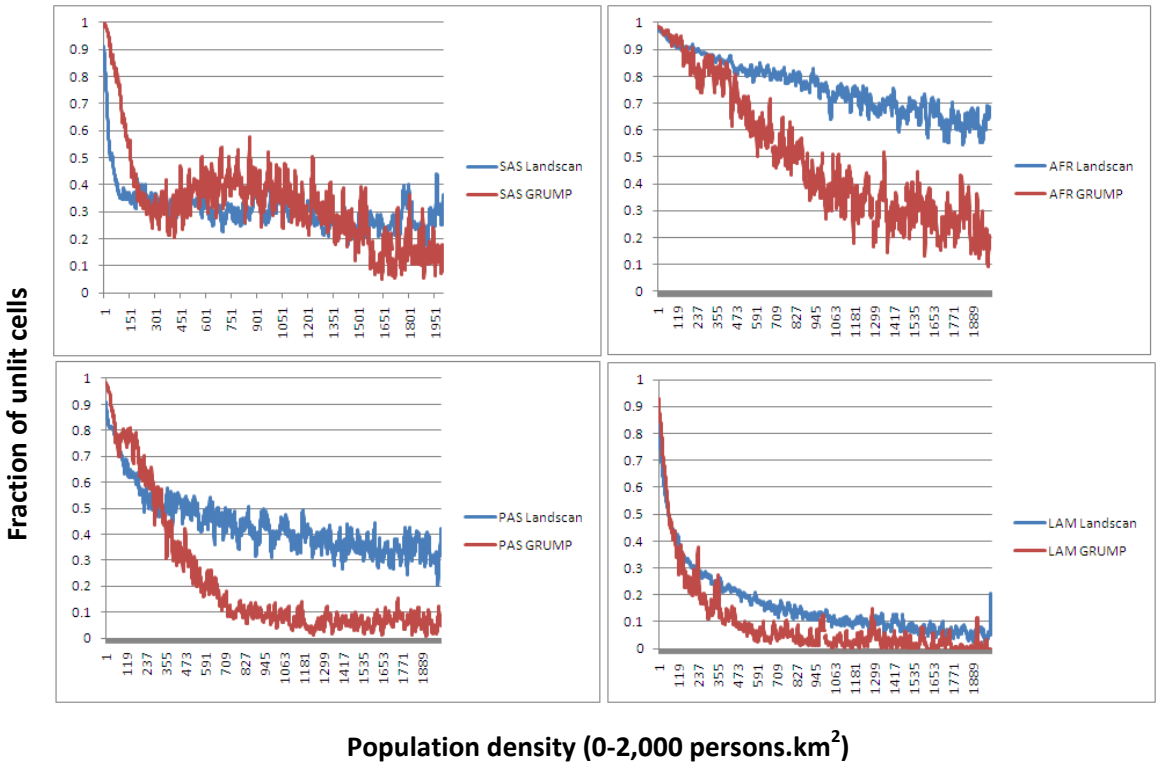

Figure 2. Population density detection profile for four regions. Clockwise from top left: SAS – South Asia; AFR – Sub-Saharan Africa; LAM – Latin America; PAS – Pacific Asia.

The final group of regions shown in Figure 3 comprise the Former Soviet Union, Centrally Planned Asia and the Middle East-North Africa plus the global average. The Former Soviet Union exhibits rapid decrease in unlit cells down to 10% at 200 persons.km^{-2} for GRUMP with LandScan lagging at 40% but converging at 700 persons.km^{-2}. Centrally Planned Asia is the only regions where GRUMP displays less coincidence with light than LandScan. LandScan settles at 70% detection from 450 persons.km^{-2} onwards, whilst GRUMP dips below that at 750 persons.km^{-2} and then declines to similar levels observed in other regions. The Middle East region have broadly coincident profiles with greater than 80% from 250 persons.km^{-2} onwards. The bottom right panel in Figure 3 is that of the global composite, where 75% detection can be claimed for both datasets from 600 persons.km^{-2}. Whilst GRUMP dips down to less than 10% unlit cells as population density increases, globally the figure is twice as high for LandScan.

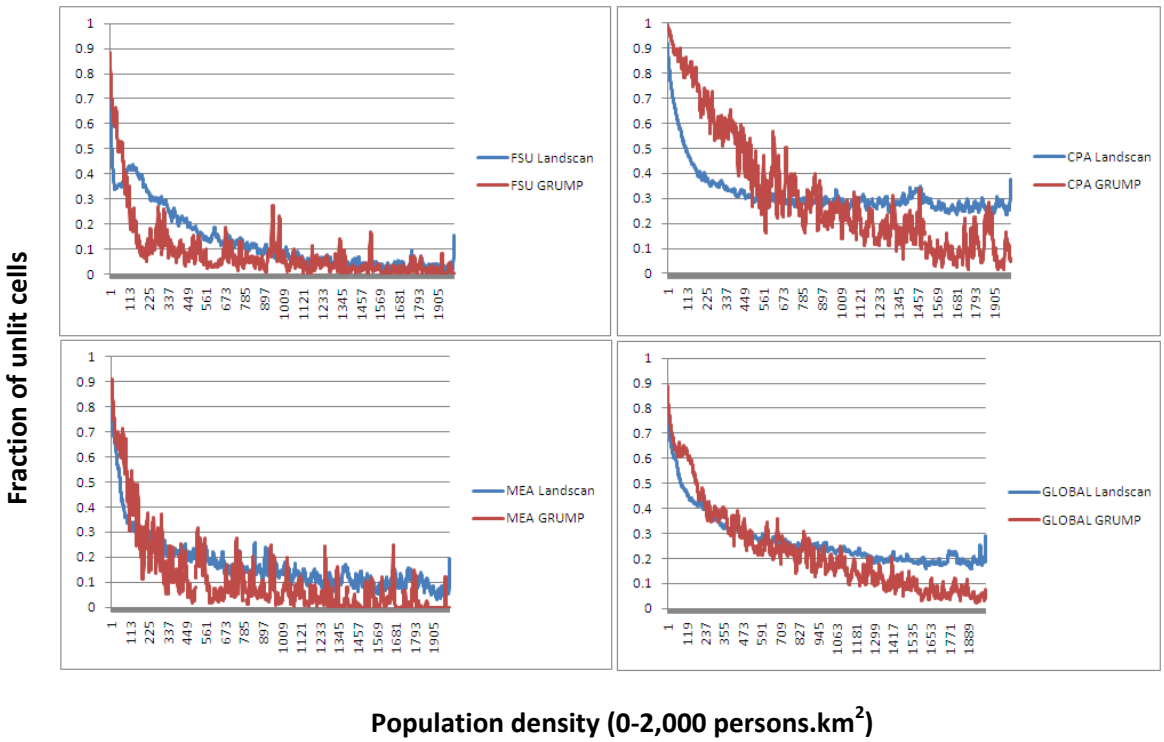

Figure 3. Population density detection profile for four regions. Clockwise from top left: FSU – Former Soviet Union; CPA – Centrally Planned Asia; Global (all regions); MEA – Middle East (incl. North Africa).

In summary, there are three main patterns that emerge:

(i) rapid decline in the fraction of unlit cells to consistently high detection levels.

(ii) decline in the fraction of unlit cells leveling off at medium levels of detection.

(iii) decline in the fraction of unlit cells followed by a shallower decline to high levels of detection (< 0.2 unlit).

Table 1 summarises the population density by region for 50% and 75% detection levels of DMSP-OLS night-time lights. Over the range of development worldwide, there is a 50% chance of detection from night-time lights for population densities ranging from 5-811 persons.km^{-2} for the GRUMP dataset and 1-2,184 persons.km^{-2} for the LandScan dataset and a 75% chance of detection for densities ranging from 11-1,611 persons.km^{-2} in GRUMP and 6-7,150 persons.km^{-2} in LandScan.

Region	GRUMP 50%	LandScan 50%	GRUMP 75%	LandScan 75%
NAM	5	1	11	6
PAO	11	7	25	17
WEU	14	1	45	15
EEU	27	2	52	16
FSU	52	16	97	341
LAM	55	54	165	316
MEA	91	49	252	266
SAS	150	39	1,417	1,308
GLOBAL	**172**	**80**	**535**	**700**
PAS	280	308	522	2,238
CPA	395	100	767	1,670
AFR	811	2,184	1,611	7,150

Table 1. Regional Population Density for GRUMP and LandScan population datasets at 50% and 75% detection levels of DMSP-OLS imagery.\

3.2. Mean population density as a function of DN

This section presents the counterpart analysis of mean population density in lit areas by plotting the weighted average of population for the lit DN values up to 63. Here we see the most developed regions of the world sharply increase in brightness with relatively small increases in population density as indicated by sharp vertical lines on the graphs. By contrast less developed regions show more gradual increases in brightness as population density increases. The LandScan dataset shows the greatest variation in population density with increasing brightness levels with the profile for South Asia especially outstanding. In each case, the average population density for the highest DN values are significantly higher due to the saturation of the DMSP-OLS sensor over bright urban areas, which has the effect of concentrating very high population densities in one brightness level. Clustering of profiles is noticeable in both datasets with the North American region standing out as having consistently lower population densities et every brightness level. For the GRUMP dataset, the other regions follow similar patterns and only diverge beyond DN=50. There are 4 regions however, which follow different paths from the outset. Sub Saharan Africa and Pacific Asia have coincident profiles along with South Asia and Centrally Planned Asia displaying the greatest increase in population density with brightness.

The pattern is similar for LandScan albeit with greater increases in population density at higher DN values. The same 4 regions identified for GRUMP follow much more even trajectories with South Asia again displaying clear increases in population density per increasing DN with Sub-Saharan Africa the next region showing the most differentiation.

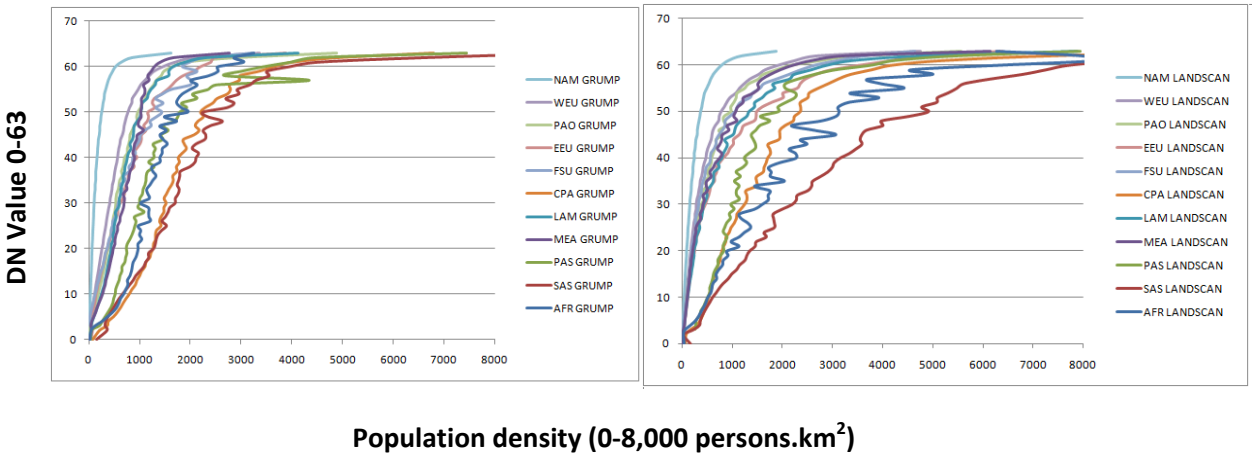

Figure 4. Average Population density per DN value for two global gridded population datasets. Left panel: CIESIN's GRUMP. Right panel: LandScan. *Source: LandScan 2008™, ORNL, UT-Battelle, LLC.*

Sample population densities for the GRUMP dataset at DN values of 0, 10, 25, 40, 50 and 63 (saturation) are show in Table 2 for comparison. Less developed regions have higher population densities for a given DN than more developed regions. That is to say, lower population densities are detected earlier in more developed regions of the world as was shown in Figures 1-3. The average population density for the regions as a whole is also shown in the last column.

DN	0	10	25	40	50	60	63	average density
NAM GRUMP	4	29	82	159	251	522	1620	53
WEU GRUMP	17	107	327	557	762	1449	3355	114
PAO GRUMP	4	184	467	702	961	1639	4879	126
MEA GRUMP	16	280	575	910	1027	1297	2771	54
LAM GRUMP	11	254	502	760	1022	1658	4115	41
CPA GRUMP	77	796	1422	1762	2200	3639	6800	155
FSU GRUMP	9	129	467	869	1444	1849	3222	31
EEU GRUMP	39	137	476	942	1160	2192	3876	109
AFR GRUMP	28	693	979	1405	1954	2547	3260	40
SAS GRUMP	153	665	1530	2113	2249	3954	9547	277

PAS GRUMP	49	527	914	1288	1794	3441	7439	126

Table 2. Typical GRUMP population densities found at DN values by region of the world.

Comparing regions of similar average population density but different development levels allows us to see what impact development has on lighting intensity. Broadly speaking, for regions of similar average population density, a less developed region has twice the population density at saturation (DN=63) than the more developed region.

4. Discussion

One reason for the discrepancy between the GRUMP and LandScan datasets is that the LandScan data makes use of many more input datasets to the allocate population. Figure 5 shows an area over the city of Kano in Nigeria. The lit areas are masked out in white, which are observed to increase between the two time periods. The most obvious difference between the two datasets is the increased detail of LandScan dataset. Whilst the GRUMP data interpolates smoothly within defined administrative regions, the LandScan dataset can be seen to contain a lot more information. In particular the LandScan algorithm used to allocate population highlights the underlying road network. In areas which have relatively low levels of lighting, this will result in population being shifted out of lit areas along transportation networks and increasing the proportion of high(er) population density cells that occur outside lit areas, which is what we observe for several regions with Pacific Asia (PAS) and Sub-Saharan Africa (AFR) the most striking over the long range (0-2,000 persons.km^{-2}).

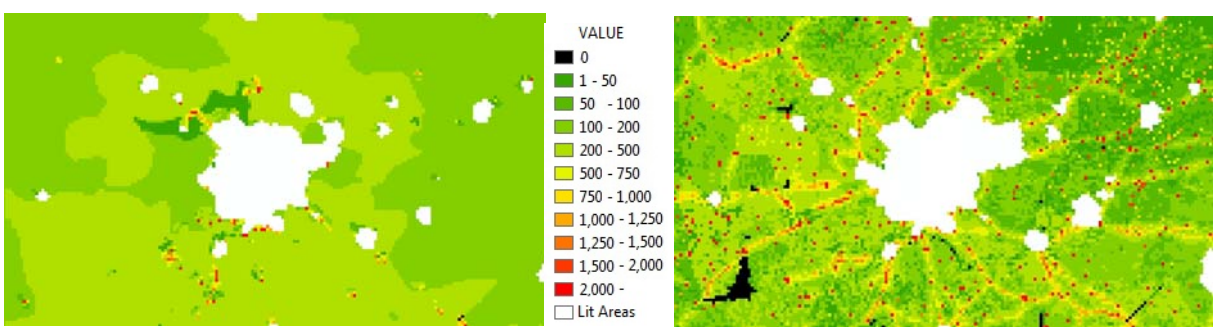

Figure 5. Comparison of Population density distribution in unlit areas over Kano, Nigeria (AFR). Left panel: CIESIN's GRUMP 2000. Right panel: LandScan. *Source: LandScan 2008™, ORNL, UT-Battelle, LLC.*

Which of the two datasets is the more accurate remains an open question. The more detailed and precise representation of population distribution in LandScan should not be taken as a proxy for accuracy. However the fact that there are only two regions (South Asia and Pacific Asia) where there is a sharp difference in the levels of detected population between the two datasets (Figure 2) may reflect the difference in the level and detail of inputs to the LandScan dataset in these two regions. As mentioned in the early part of this paper, the overglow issue was not directly addresssed in this paper. Nonetheless, we can make some comments as to what the impacts of overglow may be on the results for different regions. In highly developed regions such as North America and Western Europe overlglow is likely to be responsible for the result of high detection levels at low population densities. To illustrate this, the corresponding graph shown in the top left panel of Figure 1 for North America is shown in Figure 6 with a threshold of DN=12 applied. We observe a large shift of profiles to the right for both datasets with 50% detection levels retarded by 50 and 75 persons.km^2 for GRUMP and Landscan datasets respectively.

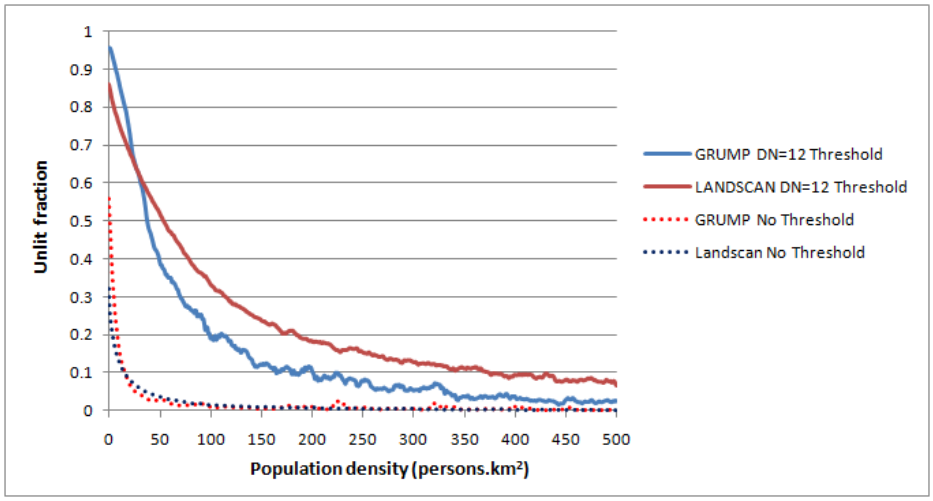

Figure 6. Comparison of unlit fractions with population density with a DN=12 threshold applied to illustrate a correction of overglow.

The problem of correcting this effect with the imposition of a simple threshold results in the attenuation of smaller lights in developing regions. Therefore an adaptive threshold is required to properly evaluate this effect. Given that overglow is a more severe effect in areas with high levels of electrification, we can assume that this offset is declines in magnitude with declining levels of economic development, however the effect could still be significant around large

settlements and megacities in the developing world. From the perspective of this study, it is considered to be less of an issue in rural areas with relatively high population densities and low levels of electrification. Although GRUMP is based in part on an early version of the lights, the extent of the 1994-95 stable lights has a far lower spatial extent than the 2000 lights used in this analysis, so whilst higher population densities occur than would otherwise be the case, there are lit areas which are less directly affected. In fact, it appears that the 1994-95 corresponds closely to the DN=12 threshold used in Figure 6 to gauge this effect.

The summary table in Table 2 shows that mean population density in DN=0 areas range from 4-153 persons.km^{-2} over the different regions of the world. Taken together with the detection rates at different population densities from the first part of the analysis, we start to build a sense of how many people we can expect to detect from night-time light imagery across the world. We also note that those 4 regions AFR, CPA, SAS, PAS which have the highest population densities for any DN values presented are also the same regions which still have around 30% of cells in unlit areas at those densities indicating that whilst a weighted average of the whole distribution of population densities present at that DN value, it may apply to around 70% of those cells and so both elements need to be considered when making assessments as two what one may assume is observable. Lower portions of Figure 4 may be disregarded depending on the threshold one takes for overglow effects.

5. Conclusions

This paper has taken two widely used and publically available population datasets and compared to the night-time light satellite imagery from the DMSP-OLS sensor by region of the world. In doing so, a greater understanding is generated on what the relative detection levels of population are from the lights according to census based population and modeled ambient population. We find that detection rates vary widely over the world. In summary, there are two main features of population detection in unlit areas.

i) In regions where differences exist between the two datasets, LandScan tends to have lower rates of detection than GRUMP for a given population density.

ii) Detection profiles follow one of two patterns:

   a. A sharp drop to steady (low) levels of the fraction of unlit cells in relation to population density.

   b. A more gradual decline, where upon detection becomes constant but not at very low levels.

Globally, 15% of population is undetected by light emission at 2,000 persons.km^{-2}, thought this can be as high as 60% in sub-saharan Africa for the LandScan dataset. Interestingly, LandScan's ambient population is usually less detected than census based GRUMP. Whilst these differences are usually small, they are pronounced in sub Saharan Africa and Pacific Asia beyond around 600 persons.km^{-2} range. Around 20% of population is still undetected in Sub-Saharan Africa and South Asia at 2000 persons.km^{-2} whereas virtually all but the lowest population density areas are detectable from light emissions in OECD countries.

Another way to consider the results is as different stages on the same path of development. Whilst one can image regions converging to the same end profile, the precise elements remain unclear as there exists a large gap in the figures for both detection and DN-density between North America and other highly developed regions. Indeed, given the pace of urbanization and changes in the cultural use of light, we may see different patterns emerge altogether. The results and analysis presented here not only assists in further studies on mapping electricity access but also provide metrics by which development may be tracked over time given the increasing availability of both nighttime light satellite data and spatially explicit socio-economic datasets. Given that overglow effects were not fully quantified but shown to be potentially significant, especially in the developed world, the results presented here should be taken as minimum values of population detection.

Acknowledgements

The author expresses sincere gratitude to Dr.Christopher Elvidge for the opportunity to present and contribute to APAN30 meeting in Hanoi and more generally to the team at NOAA-NGDC for processing, developing and distributing the DMSP-OLS night-time lights dataset. The author is also grateful to the constructive comments from three anonymous reviewers.

References

1. Doll, C.N.H; Pachauri, S. Estimating rural populations without access to electricity in developing countries through night-time light satellite imagery. *Energy Policy* ***2010,*** 38, 5661–5670

2. Elvidge, C.D; Baugh, K.E; Sutton, P.C; Bhaduri, B; Tuttle, B.T; Ghosh, T; Ziskin, D; Erwin, E.H. Who's in the dark—satellite based estimates of electrification rates. In: *Urban*

Remote Sensing: Monitoring, Synthesis and Modeling in the Urban Environment. Ed. Yang, X.Wiley-Blackwell, Chichester, UK. 2010.

3. Sutton, P.C; Roberts, D; Elvidge, C; Baugh, K. Census from Heaven: an estimate of the global human population using night-time satellite imagery. *International Journal of Remote Sensing*, ***2001.*** 22 (16) 3061 – 3076

4. Sutton, P.C; Elvidge, C.D; Obremski, T. Building and evaluating models to estimate population density. *Photogrammetric Engineering and Remote Sensing.* ***2003,*** 69(5), 545-553.

5. Sutton, P; Roberts, D; Elvidge, C; Meij, H. A comparison of nighttime satellite imagery and population density for the continental United States. *Photogrammetric Engineering and Remote Sensing.* ***1997***, 63(11), 1303-1313.

6. Raupach, M.R; Rayner, P.J; Paget, M. Regional variations in spatial structure of nightlights, population density and fossil-fuel CO_2 emissions. *Energy Policy* ***2010,*** 38, 4756-4764

7. IIASA. GGI Database. 2006. Available at: http://www.iiasa.ac.at/web-apps/ggi/GgiDb/dsd?Action=htmlpage&page=about#acronyms

8. NOAA-NGDC. Version 4 DMSP-OLS Nighttime Lights Time Series. ***2010***. Available online from: http://www.ngdc.noaa.gov/dmsp/downloadV4composites.html

9. Elvidge, C.D; Baugh, K.E; Kihn, E.A; Kroehl, H.W. and Davis, E.R; Mapping city lights with nighttime data from the DMSP operational linescan system. *Photogrammetric Engineering and Remote Sensing*, ***1997***, 63 (6), 727-734.

10. Elvidge, C.D; Imhoff; M.L; Baugh, K.E; Hobson, V-R; Nelson; I; Safran, J; Dietz, J.B. and Tuttle; B.T; Night-time lights of the world: 1994-1995. *ISPRS Journal of Photogrammetry & Remote Sensing*, ***2001,*** 56, 81-99

11. Elvidge, C.D; Baugh, K.E; Dietz, J.B; Bland, T; Sutton, P.C; Kroehl, H.W. Radiance calibration of DMSP-OLS low-light imaging data of human settlements. *Remote Sensing of Environment.* ***1999***, 68 (1), 77-88.

12. Small, C., Pozzi, F. C. D. Elvidge, C.D. 2005. Spatial analysis of global urban extent from DMSP-OLS night lights. Remote Sensing of Environment (96) 277-291

13. Center for International Earth Science Information Network (CIESIN), Columbia University; International Food Policy Research Institute (IFPRI); The World Bank; and Centro Internacional de Agricultura Tropical (CIAT), Global Rural–UrbanMapping Project (GRUMP), Alpha Version: Coastlines. Socioeconomic Data and Applications Center

(SEDAC), **2004,** Columbia University, Palisades, NY. Available at: http://sedac.ciesin.columbia.edu/gpw

14. LandScan (2008)™ High Resolution global Population Data Set copyrighted by UT-Battelle, LLC, operator of Oak Ridge National Laboratory under Contract No. DE-AC05-00OR22725 with the United States Department of Energy. The United States Government has certain rights in this Data Set. Neither UT-BATTELLE, LLC NOR THE UNITED STATES DEPARTMENT OF ENERGY, NOR ANY OF THEIR EMPLOYEES, MAKES ANY WARRANTY, EXPRESS OR IMPLIED, OR ASSUMES ANY LEGAL LIABILITY OR RESPONSIBILITY FOR THE ACCURACY, COMPLETENESS, OR USEFULNESS OF THE DATA SET.

15. Bhaduri, B; Bright, E; Coleman, P; Dobson, J; LandScan: Locating people is what matters. ***Geoinformatics 2002***, 5, 34-37

16. ORNL, LandScan documentation. ***2010***. Available from: http://www.ornl.gov/sci/LandScan/LandScan_documentation.shtml

Accepted October 14, 2010
Published December 31, 2010

© 2010 by the authors; licensee Asia Pacific Advanced Network. This article is an open-access article distributed under the terms and conditions of the Creative Commons Attribution license (http://creativecommons.org/licenses/by/3.0/).